

# UC Santa Barbara

## UC Santa Barbara Previously Published Works

### Title

Model-free test of local-density mean-field behavior in electric double layers

### Permalink

<https://escholarship.org/uc/item/7z8434zc>

### Journal

Physical Review E - Statistical, Nonlinear, and Soft Matter Physics, 88(1)

### ISSN

1539-3755

### Authors

Giera, B  
Henson, N  
Kober, EM  
[et al.](#)

### Publication Date

2013-07-29

### DOI

10.1103/PhysRevE.88.011301

Peer reviewed

## Model-free test of local-density mean-field behavior in electric double layers

Brian Giera,<sup>1</sup> Neil Henson,<sup>2</sup> Edward M. Kober,<sup>2</sup> Todd M. Squires,<sup>1</sup> and M. Scott Shell<sup>1</sup>

<sup>1</sup>*Department of Chemical Engineering, University of California Santa Barbara, Santa Barbara, California 93106, USA*

<sup>2</sup>*Los Alamos National Laboratory, Los Alamos, New Mexico 87545, USA*

(Received 19 January 2013; published 29 July 2013)

We derive a self-similarity criterion that must hold if a planar electric double layer (EDL) can be captured by a local-density approximation (LDA), without specifying any specific LDA. Our procedure generates a similarity coordinate from EDL profiles (measured or computed), and all LDA EDL profiles for a given electrolyte must collapse onto a master curve when plotted against this similarity coordinate. Noncollapsing profiles imply the inability of any LDA theory to capture EDLs in that electrolyte. We demonstrate our approach with molecular simulations, which reveal dilute electrolytes to collapse onto a single curve, and semidilute ions to collapse onto curves specific to each electrolyte, except where size-induced correlations arise.

DOI: [10.1103/PhysRevE.88.011301](https://doi.org/10.1103/PhysRevE.88.011301)

PACS number(s): 07.05.Tp, 82.45.-h, 61.20.Qg, 82.47.Uv

Nanoscale electric double layers (EDLs) form at all interfaces between charged surfaces (including electrodes [1], colloids [2], proteins [3], and cell membranes [4]) and electrolytes [5] or ionic liquids [6]. EDLs form due to the competition between electrostatic attraction of oppositely charged counterions towards the interface, and osmotic repulsion down resulting concentration gradients. EDLs play a central role in colloidal suspensions [7,8], polyelectrolytes [9], micro- and nanofluidics [10,11], and in supercapacitors [12,13] that store energy electrochemically across the EDL. The EDL structure governs differential capacitance [14], electrokinetic flow [15–17], surface conductivity [18], capacitive desalination [19–21], and rational design of EDLCs [22,23].

For over a century, EDL structure has been almost universally modeled using the Poisson-Boltzmann equation (PBE), which takes the form

$$\lambda_D^2 \nabla^2 \left( \frac{qe\phi}{k_B T} \right) = \frac{n_- - n_+}{2n^B} = \sinh \left( \frac{qe\phi}{k_B T} \right), \quad (1)$$

for binary electrolytes, but can easily be generalized for multiple ion species and valences [7]. Here  $\phi$  is the electrostatic excess chemical potential relative to the bulk,  $\lambda_D = (8\pi\lambda_B n^B)^{-1/2}$  is the Debye “screening” length,  $n^B = n_+^B = n_-^B$  is the bulk ion density, and  $\lambda_B = (qe)^2 / (4\pi\epsilon k_B T)$  is the Bjerrum length, beyond which thermal energy  $k_B T$  exceeds the electrostatic energy between charges  $\pm qe$  in a uniform continuum with permittivity  $\epsilon$ . The PBE (1), solved for planar EDLs by Gouy and Chapman (GC) [24,25], assumes ideal, pointlike ions that establish (and respond to) a mean electric field in a structureless, continuum solvent.

Despite its near-ubiquitous use, the GC theory (and PBE more generally) has long been known to fail for various reasons. Boltzmann-distributed densities grow exponentially with  $\phi$ , predicting ions of diameter  $\sigma$  that can exceed close packing [26,27]. Experiments [1,28] and computations [29,30] suggest inherently non-PBE effects due to ion shape [8,31], solvation [32,33], size- [6,34] and electrostatically induced ordering [35–40], dielectric inhomogeneities [41–43], and physicochemical [44–46] and discrete charge [47,48] wall-ion interactions.

Nonetheless, the PBE (1) remains appealing since it can be solved rapidly for systems and geometries that would be

far larger than atomistic simulations would allow. A sustained search for modified PBEs has thus ensued [28], seeking to preserve the local, mean-field assumptions that give simple PDEs such as (1), while accounting for phenomena beyond PB and GC. Widely used local-density approximations (LDAs) assume ions to respond to additional interactions that depend *only* on local ion densities, with “excess” chemical potential  $\mu_{\pm}^{\text{ex}}(n_i)$ , as in bulklike systems [28,49]. Wall-ion interactions  $\mu_{\pm}^{\text{wall}}(z)$  may also be included in the Boltzmann distribution,

$$n_{\pm} = n_{\pm}^B \exp \left( \mp \frac{qe\phi}{k_B T} - \frac{\mu_{\pm}^{\text{ex}}(n_i)}{k_B T} - \frac{\mu_{\pm}^{\text{wall}}(z)}{k_B T} \right), \quad (2)$$

or additional ion species, which are then used in (1) to yield a modified PBE. LDAs have been used to treat short-ranged enthalpic [3,50] and steric interactions between equisized [26,27] and asymmetric [51] ions, and to model ionic liquids [6], electrochemical cells [20], and ion density profiles from x-ray reflectivity measurements of liquid-liquid interfaces [5] and Langmuir monolayers [52].

Despite their appealing simplicity, there is no reason to expect *a priori* that any LDA can accurately describe EDLs in a particular electrolyte [40]. For example, molecular simulations have revealed strong dielectric inhomogeneities [53], which continuum EDL theories have treated using integro-differential equations [53] or Ginzburg-Landau expansions [54]; neither is compatible with a LDA theory. LDAs neglect structuring effects due to ion-surface, ion-ion, and ion-solvent correlations that may be significant in actual EDLs [40]. Increasingly powerful atomistic simulations can reveal EDL features for specific ion and solvent chemistries [55], but are typically impractically expensive for even moderate size or time scales. Ideally, a continuum theory could be developed for large-scale modeling that nonetheless respects the physicochemical properties of a specific electrolyte, e.g., by incorporating  $\mu_{\pm}^{\text{ex}}$  obtained from molecular simulations or measurements into a LDA.

Current LDA searches assume some (physically motivated) form of  $\mu_{\pm}^{\text{ex}}$  and then assess the consequences. If a particular  $\mu_{\pm}^{\text{ex}}$  fails to capture measured or simulated EDL behavior, however, one does not know whether a different choice might succeed, or whether the LDA approach is itself bound to fail. It is thus crucial to know whether an EDL can possibly be

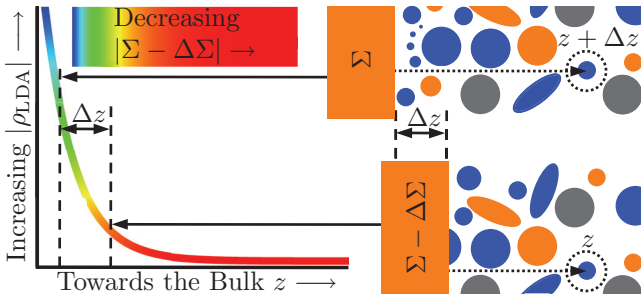


FIG. 1. (Color online) Universality of local-density approximation electric double layers: Any ion located a distance  $z + \Delta z$  from an interface of surface charge density  $\Sigma$  (top right) would “feel” no different than were the interface located a distance  $\Delta z$  closer (bottom right) with lower effective surface charge density  $\Sigma - \Delta\Sigma$  given by Eq. (3). All LDA EDLs represent a portion of a single, universal charge density profile  $\rho_{\text{LDA}}$  (left).

captured by any LDA—and therefore whether a simple PDE can be derived for its description in more complex geometries and systems.

Here, we develop a “model-free” method that can be used to systematically determine whether it is possible for any LDA to describe EDLs in a particular electrolyte. We start with a deceptively simple question: Does an ion in an EDL “know” the location of the surface (Fig. 1)? In any LDA EDL, an ion located a distance  $z$  from a surface with charge density  $\Sigma$  would behave the same if a less-charged surface were  $\Delta z$  closer, provided that the effective charge density  $\Sigma_{\text{eff}}$  at  $\Delta z$  obeyed

$$\Sigma_{\text{eff}} = \Sigma - \Delta\Sigma = \Sigma + \int_0^{\Delta z} \rho(\tilde{z}, \Sigma) d\tilde{z}. \quad (3)$$

More formally, any LDA description yields an EDL whose free charge density  $\rho = qe(n_+ - n_-)$  falls onto a single, master curve  $\rho(z, \Sigma)$ . LDA EDL density profiles, each with a different  $\Sigma$ , can thus be shifted by some  $\Delta z$  ( $\Delta\Sigma$ ) to fit onto the universal EDL profile.

This self-similarity enables an equation for the universal EDL curve for any local-density approximation to be derived explicitly, since charge densities in differently charged LDA EDLs obey the underlying self-similarity

$$\rho(z, \Sigma) = \rho(z + \Delta z, \Sigma + \Delta\Sigma), \quad (4)$$

where  $\Delta\Sigma$  and  $\Delta z$  are related via Eq. (3). For small  $\Delta\Sigma$  and  $\Delta z$ , the Taylor expansion of (4) and  $\Delta\Sigma/\Delta z = -\rho(0, \Sigma)$  via (3) combine to give a self-consistency equation,

$$\left. \frac{\partial \rho}{\partial z} \right|_{\Sigma} = \left. \frac{\partial \rho}{\partial \Sigma} \right|_z \rho(0, \Sigma). \quad (5)$$

Any EDL that obeys a LDA—regardless of the specific  $\mu_{\pm}^{\text{ex}}(n_i)$ —must obey Eq. (5). Conversely, comparing simulated or measured EDL profiles against (5) directly reveals whether any simple LDA  $\mu_{\pm}^{\text{ex}}$  can possibly exist that successfully captures that EDL. Ion-wall interactions  $\mu_{\pm}^{\text{wall}}(z)$  do not obey this relation, but the arbitrariness of “ $z = 0$ ” allows (5) to be used with an effective origin chosen to lie beyond the ion-wall interaction range.

The free charge density  $\rho$  can be derived explicitly from (5) using the method of characteristics, provided  $\rho(0, \Sigma)$  is known, measured, or simulated. Furthermore,  $\rho$  depends only on a similarity variable  $S(z, \Sigma; \dots)$ , given by

$$S = \tilde{\Sigma} \exp\left(-\tilde{z} - \int_0^{\tilde{\Sigma}} \left[ \frac{1}{\tilde{\rho}(0, \tilde{\Sigma}; \dots)} + \frac{1}{\tilde{\Sigma}} \right] d\tilde{\Sigma}\right), \quad (6)$$

where we use nondimensionalized variables  $\tilde{z} = z/\lambda_D$ ,  $\tilde{\rho} = (\lambda_D/\Sigma_{\text{ref}})\rho$ , and  $\tilde{\Sigma} = \Sigma/\Sigma_{\text{ref}}$ , where  $\Sigma_{\text{ref}} = qe/(4\pi\lambda_B\lambda_D)$  [56]. The charge density is then given by

$$\tilde{\rho}(S) = \tilde{\rho}(\tilde{z} = 0, \tilde{\Sigma} = g^{-1}[S]), \quad (7)$$

where  $g[\tilde{\Sigma}] = \tilde{\Sigma} \exp(-\int_0^{\tilde{\Sigma}} [1/\tilde{\rho}(0, \tilde{\Sigma}; \dots) + 1/\tilde{\Sigma}] d\tilde{\Sigma})$ .

Given the free charge density at contact,  $S$  can be solved explicitly and embeds physical quantities such as ion size  $\sigma$ , screening length  $\lambda_D$ , electrostatic strength  $\lambda_B$ , distance  $z$ , and surface charge density  $\Sigma$ .  $S$  then collapses LDA EDLs in a given electrolyte onto a single master curve.

The Debye-Hückel (DH) limit, valid for low EDL potentials  $\phi \ll k_B T/qe$  and negligible excess contributions  $\mu_{\pm}^{\text{ex}} \rightarrow 0$ , provides an instructive example. In this restrictive regime, the linearized Eq. (1) gives  $\tilde{\rho}_{\text{DH}}(0, \tilde{\Sigma}) = -\tilde{\Sigma}$  [7], and Eqs. (6) and (7) can be solved explicitly to give  $S_{\text{DH}} = \tilde{\Sigma} \exp(-\tilde{z})$  and  $\tilde{\rho}_{\text{DH}} = -S_{\text{DH}}$ . Beyond the linear regime, the Gouy-Chapman contact expression  $\rho_{\text{GC}}(0, \Sigma)$  [57] yields an analytical similarity variable that measures the mean-field strength between an electrified plate and uncorrelated point-sized ions,

$$S_{\text{GC}} = \left( \frac{2}{1 + \sqrt{1 + (\tilde{\Sigma}/2)^2}} \right) \tilde{\Sigma} e^{-\tilde{z}}, \quad (8)$$

that reduces to  $S_{\text{DH}}$  for  $\tilde{\Sigma} \ll 1$ . Notably,  $S_{\text{GC}}$  varies continuously between two limiting behaviors: (i)  $S_{\text{GC}} \rightarrow S_{\text{DH}} \rightarrow 0$  far from weakly charged surfaces ( $\tilde{z} \rightarrow \infty, \tilde{\Sigma} \rightarrow 0$ ), and (ii)  $S_{\text{GC}} \rightarrow 4$  near strongly charged surfaces ( $\tilde{z} \rightarrow 0, \tilde{\Sigma} \rightarrow \infty$ ). The GC free charge density,

$$\tilde{\rho}_{\text{GC}} = \frac{\rho_{\text{GC}}}{2qen^{\text{B}}} = -\frac{16S_{\text{GC}}(16 + S_{\text{GC}}^2)}{(16 - S_{\text{GC}}^2)^2}, \quad (9)$$

thus diverges in the  $S_{\text{GC}} \rightarrow 4$  limit,  $\tilde{\rho}_{\text{GC}} \rightarrow \tilde{\rho}_{\text{DH}}$  for  $S_{\text{GC}} \ll 1$ , and approaches electroneutrality ( $\tilde{\rho}_{\text{GC}} \rightarrow 0$ ) as  $S_{\text{GC}} \rightarrow 0$ .

Having derived Eq. (5)—a general, model-free condition that must be satisfied for any planar EDL describable by LDAs—we now use molecular dynamics to explicitly simulate ions within fully formed EDLs for which LDA physics is by no means guaranteed. To focus on the general applicability of our results, we employ the simplest model for ions that captures many-body interactions, rather than using force fields and characteristics specific to a particular electrolyte system. Specifically, we use LAMMPS [58] to simulate primitive model (PM) electrolytes: charge-centered Weeks-Chandler-Andersen [59] ions of diameter  $\sigma_{\text{WCA}}$  and charge  $\pm qe$  in an implicit Langevin solvent [60] with constant permittivity  $\epsilon$ , bound by uniformly charged repulsive 9/3 surfaces separated by a distance  $L$  in a  $xy$ -periodic system. Defining system parameters gives three physical length scales: the Bjerrum length  $\lambda_B$  that reflects ion valence, permittivity, and thermal energy; the screening length  $\lambda_D$ , which is measured from

equilibrated bulk ion concentrations; and the effective hard-core ion diameter  $\sigma \approx 0.95\sigma_{\text{WCA}}$  that sets the bulk volume fraction  $\Phi^{\text{B}} = \sigma^3/(24\lambda_{\text{B}}\lambda_{\text{D}}^2)$  [56]. We choose the system size  $L$  to be large enough by comparison to be irrelevant. Nondimensionalizing lengths by  $\lambda_{\text{D}}$  reveals any PM electrolyte and surface to be uniquely specified by three dimensionless parameters:  $\Phi^{\text{B}}$ ,  $\lambda_{\text{B}}/\lambda_{\text{D}}$ , and  $\tilde{\Sigma}/\Sigma_{\text{ref}}$ .

For each PM electrolyte  $\{\Phi^{\text{B}}; \lambda_{\text{B}}/\lambda_{\text{D}}\}$  and surface charge  $\tilde{\Sigma}$ , we equilibrate  $O(800\text{--}1400)$  ions for 5 000 000 MD time steps, then evenly collect 50 000 snapshots over 50 000 000 steps, requiring 50–100 CPU hours per run. We then measure the time-averaged free charge density and effective local surface charge versus distance  $\tilde{z}$  from the wall, and regression fit  $\tilde{\rho}_{\text{PM}}(\tilde{z})$  vs  $\tilde{\Sigma}_{\text{eff}}(\tilde{z})$  to determine  $\tilde{\rho}_{\text{PM}}(0, \tilde{\Sigma})$ . We then use (6) to obtain a similarity variable  $S_{\text{PM}}(\tilde{z}, \tilde{\Sigma})$ . If any viable LDA theory exists for that electrolyte  $\{\Phi^{\text{B}}; \tilde{\lambda}_{\text{B}}\}$ , then computed  $\tilde{\rho}_{\text{PM}}$  profiles, replotted against  $S_{\text{PM}}$ , must collapse onto a master curve.

Figure 2 shows EDL profiles computed in seven distinct PM electrolytes with ions from low to moderate valence ( $0.05 \lesssim \lambda_{\text{B}}/\lambda_{\text{D}} \lesssim 1$ ) and very low volume fractions  $\Phi^{\text{B}} \leq 8 \times 10^{-4}$ , each for 100 distinct surface charge densities ( $0 \leq \tilde{\Sigma} \lesssim 10$ ) and measured at 250 distinct positions [56]. Under these dilute conditions, one would expect the PB-GC theory to hold, especially at small  $\tilde{\sigma}$ ,  $\tilde{\lambda}_{\text{B}}$ , and  $\tilde{\Sigma}$ . Indeed,  $\tilde{\rho}_{\text{PM}}$  collapses when plotted against  $S_{\text{PM}}$  [Fig. 2(a)], and also against  $\tilde{\Sigma}_{\text{eff}}$

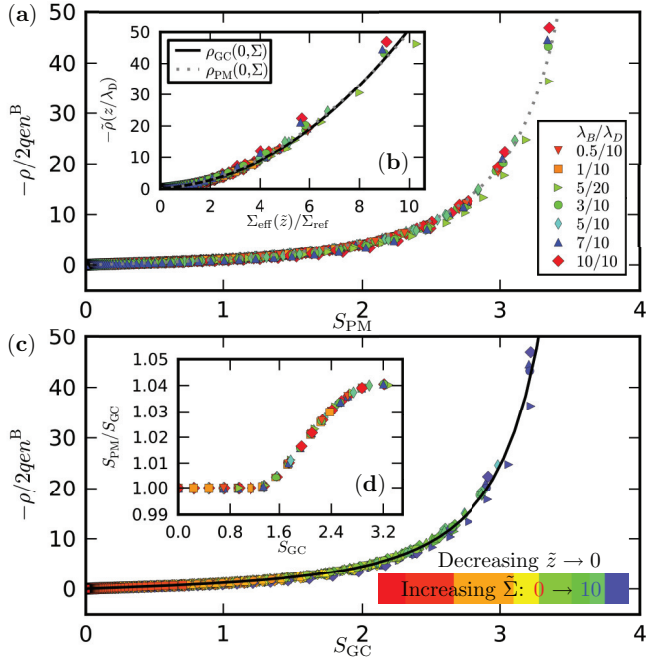


FIG. 2. (Color online) MD simulations of dilute primitive model electrolytes ( $\Phi^{\text{B}} \leq 8 \times 10^{-4}$ ) show underlying LDA behavior. (a) For a wide range of conditions, free charge density profiles all collapse onto a universal curve, when plotted against a similarity coordinate  $S_{\text{PM}}$ , which is derived from (6) using  $\rho_{\text{PM}}(0, \Sigma)$  obtained from simulation data. (b) The charge density  $\rho(z, \Sigma)$  collapses when plotted against  $\Sigma_{\text{eff}}(z)$ , which is itself indicative of LDA behavior. (c) The Gouy-Chapman similarity variable (8) also collapses simulation data well. (d) The similarity variables  $S_{\text{PM}}$  and  $S_{\text{GC}}$ , independently derived, are practically indistinguishable for  $S_{\text{GC}} \lesssim 0.4$ , and differ by less than 4% for  $1.6 < S_{\text{GC}} \lesssim 3.2$ .

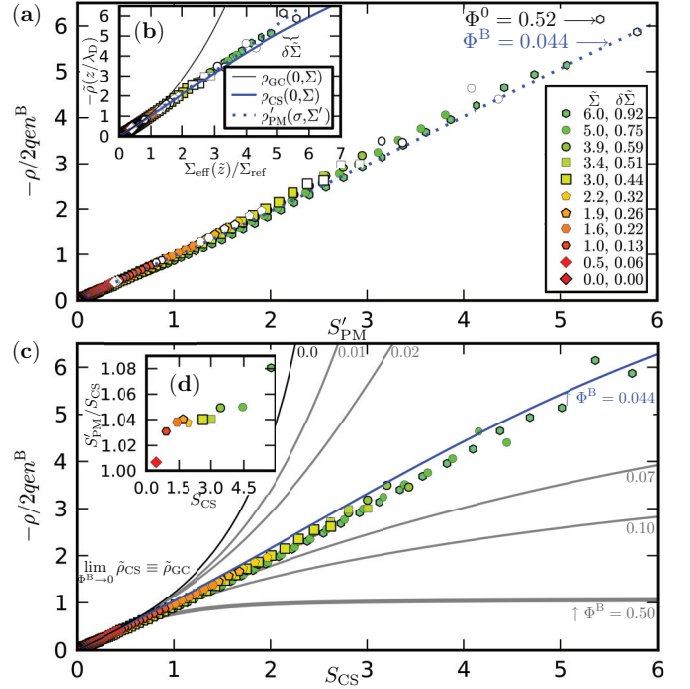


FIG. 3. (Color online) MD simulations of PM electrolytes with large ( $\sigma/\lambda_{\text{D}} \simeq 3/15$ ), weakly charged ( $\lambda_{\text{B}}/\lambda_{\text{D}} \simeq 0.1/15$ ) ions at constant bulk volume fraction  $\Phi^{\text{B}} = 0.044 \pm 0.001$  show LDA behavior beyond a surface monolayer (with packing fraction  $\Phi^0$ ). (a) Charge density profiles for various surface charge densities  $\tilde{\Sigma}$  collapse onto a single curve when plotted against  $S'_{\text{PM}}$ , obtained by evaluating (6) using measured data. (b) EDL density profiles collapse when plotted against  $\tilde{\Sigma}_{\text{eff}}$  that is reduced by the measured charge density of the monolayer  $\delta\tilde{\Sigma}$ . (c) The similarity coordinate  $S_{\text{CS}}$  generated using the LDA-Carnahan-Starling approach also collapses simulated density profiles beyond the correlated region. A one-parameter ( $\Phi^{\text{B}}$ ) family of universal EDL curves is generated from (6) and (7) using the LDA-CS approach. (d) The theoretical  $S_{\text{CS}}$  matches the measured  $S'_{\text{PM}}$  to within 10% for these simulations.

[Fig. 2(b)]. Furthermore, even *different* electrolytes collapse onto the *same* curve, irrespective of the specific electrolyte properties  $\{\Phi^{\text{B}}; \tilde{\lambda}_{\text{B}}\}$ , as is true for GC theory. In fact, the GC similarity variable  $S_{\text{GC}}$  (8) captures the observed universal profile very well [Fig. 2(c)], and closely matches the computed, model-free  $S_{\text{PM}}$  [Fig. 2(d)].

Next, we simulate semidilute electrolytes with weakly charged but moderately sized PM ions ( $\lambda_{\text{B}} \ll \sigma < \lambda_{\text{D}}$ ), where we suspect GC will fail due to finite-sized effects. We then determine whether such non-GC EDLs can nonetheless be captured by LDAs using our model-free method (Fig. 3). For these ions, specific wall-ion interactions drive surface ion monolayers to form at high  $\tilde{\Sigma}$  and/or  $\Phi^{\text{B}}$ . Since our model-free test holds outside the range of specific wall-ion interactions, we define “ $\tilde{z} = 0$ ” in Eq. (6) to lie beyond the surface ion monolayer,  $\tilde{z} > \sigma/\lambda_{\text{D}}$ , and adopt a reduced applied surface charge density  $\tilde{\Sigma}' = \tilde{\Sigma} - \delta\tilde{\Sigma}$ , where  $\delta\tilde{\Sigma} = \int_{\tilde{z}}^0 \tilde{\rho}_{\text{PM}} d\tilde{z}$  corrects for the monolayer charge. Indeed, Fig. 3(b) shows density profiles  $\tilde{\rho}'(\tilde{z} = \tilde{\sigma}, \tilde{\Sigma}'; \Phi^{\text{B}} = 0.044)$  for 11 simulations that collapse onto a single curve when plotted against  $\tilde{\Sigma}'_{\text{eff}}$  and the similarity variable  $S'_{\text{PM}}$ . Despite GC breakdown, our test

reveals EDLs in these electrolytes to obey some underlying LDA model.

Motivated by the existence of a viable LDA theory, we consider the Carnahan-Starling [61] (CS) hard-sphere model that accounts for excess hard-sphere repulsions  $\mu_{\text{CS}}^{\text{ex}}(\Phi)$  using the local volume fraction [7,28] of same sized ions. Evaluating the computed contact expression  $\tilde{\rho}_{\text{CS}}(\tilde{z} = 0, \tilde{\Sigma}; \Phi^{\text{B}})$ , we calculate  $S_{\text{CS}}(\tilde{z}, \tilde{\Sigma}; \Phi^{\text{B}})$  via (6) [56], and generate a family of universal curves for different  $\Phi^{\text{B}}$  in Fig. 3(c). The LDA-CS theory correctly produces the universal curve onto which the EDLs simulated with  $\bar{\Phi}^{\text{B}} \simeq 0.044$  collapse against  $\tilde{\Sigma}_{\text{eff}}$  [Fig. 3(b)]—but only up to a point, beyond which collapse is lost due to nonlocal ordering adjacent to the surface. The LDA-CS approach misses the oscillatory portions of PM EDLs, as any LDA would, but decently captures the mean-field strength of steric interactions in noncorrelated EDL regimes.

In summary, we have presented a general and powerful formalism to identify and elucidate local-density approximation behavior in planar EDLs, following a simple observation: LDA ions do not know the interface location. Our model-free approach enables EDL profiles—whether simulated or measured—to be directly analyzed, and to determine whether any LDA can possibly succeed. In the regimes where the computed  $S$  does not collapse the EDL profiles, any search for a LDA will be fruitless.

We have here focused on the simplest, nontrivial class of electrolytes: equisized ions of equal and opposite valence in a homogeneous, implicit solvent. It is completely straightforward to apply our model-free approach, however, to much more general electrolytes. The simplest extension

would involve asymmetric electrolytes—with two (or more) ion species of different size and valence. In that case, one can anticipate that some  $\mu_{\pm}^{\text{ex}}(\Phi_{\pm})$  [51], analogous to  $\mu_{\text{CS}}^{\text{ex}}$  for equisized ions, could be found to work in a trial LDA. No obvious  $\mu_{\pm}^{\text{ex}}$ , however, exists for less straightforward electrolytes—e.g., measured or computed with explicit solvent and specific chemical force fields. Nonetheless, our model-free test will immediately reveal whether any LDA can be found that captures such EDL behavior.

Similarity variables from distinct LDAs have distinct functional forms. For example,  $S_{\text{GC}}$  (which collapses pointlike EDL profiles) diverge, whereas  $S_{\text{CS}}$  (which collapses semidilute EDL profiles) do not. Any difference in  $S$  observed between anodic and cathodic EDLs immediately reveals anions and cations to have unequal size and/or valence. Indeed, these model-free similarity variables may serve as “fingerprints” specific to that particular electrolyte. Our approach is broadly applicable to EDL profiles from simulations, x-ray reflectivity measurements, etc., and will be valuable in assessing potential LDA behavior in more general electrolytes, e.g., where solvation effects, electrostatic correlations, or discrete interfacial charges play a significant role.

Lastly, the model-free test holds for planar EDLs, which are (fortunately) the easiest to compute and measure. Irrespective, the results of the approach presented here hold for more general geometries. We expect that once a LDA is revealed to be possible for a given electrolyte, and the corresponding  $\mu_{\pm}^{\text{ex}}(n_i)$  determined, the modified PBE derived using the appropriate LDA [Eqs. (1) and (2)] should hold as a three-dimensional PDE, valid for more general geometries.

- 
- [1] J. N. Israelachvili, *Intermolecular and Surface Forces* (Academic, London, 1992).
- [2] M. Quesada-Pérez, E. González-Tovar, A. Martín-Molina, M. Lozada-Cassou, and R. Hidalgo-Álvarez, *ChemPhysChem* **4**, 234 (2003).
- [3] P. Grochowski and J. Trylska, *Biopolymers* **89**, 93 (2007).
- [4] D. Andelman, in *Handbook of Biological Physics*, edited by R. Lipowsky and E. Sackmann, Vol. 1 (Elsevier, New York, 1995), pp. 603–642.
- [5] G. Luo, S. Malkova, J. Yoon, D. Schultz, B. Lin, M. Meron, I. Benjamin, P. Vanýsek, and M. Schlossman, *Science* **311**, 216 (2006).
- [6] A. A. Kornyshev, *J. Phys. Chem. B* **111**, 5545 (2007).
- [7] W. B. Russel, D. A. Saville, and W. R. Schowalter, *Colloidal Dispersions* (Cambridge University Press, Cambridge, UK, 1989).
- [8] J.-P. Hansen and H. Lowen, *Annu. Rev. Phys. Chem.* **51**, 209 (2000).
- [9] V. Vlachy, *Annu. Rev. Phys. Chem.* **50**, 145 (1999).
- [10] R. B. Schoch, J. Han, and P. Renaud, *Rev. Mod. Phys.* **80**, 839 (2008).
- [11] F. H. J. van der Heyden, D. Stein, K. Besteman, S. G. Lemay, and C. Dekker, *Phys. Rev. Lett.* **96**, 224502 (2006).
- [12] B. E. Conway, *Electrochemical Supercapacitors: Scientific Fundamentals and Technological Applications* (Plenum, New York, 1999).
- [13] P. Simon and Y. Gogotsi, *Nat. Mater.* **7**, 845 (2008).
- [14] M. V. Fedorov and A. A. Kornyshev, *J. Phys. Chem. B* **112**, 11868 (2008).
- [15] T. Squires and M. Bazant, *J. Fluid Mech.* **509**, 217 (2004).
- [16] R. R. Netz, *Phys. Rev. Lett.* **91**, 138101 (2003).
- [17] F. H. J. van der Heyden, D. Stein, and C. Dekker, *Phys. Rev. Lett.* **95**, 116104 (2005).
- [18] R. J. Messinger and T. M. Squires, *Phys. Rev. Lett.* **105**, 144503 (2010).
- [19] P. M. Biesheuvel and M. Z. Bazant, *Phys. Rev. E* **81**, 031502 (2010).
- [20] R. A. Rica, R. Ziano, D. Salerno, F. Mantegazza, and D. Brogioli, *Phys. Rev. Lett.* **109**, 156103 (2012).
- [21] R. Zhao, M. van Soestbergen, H. Rijnaarts, A. van der Wal, M. Bazant, and P. Biesheuvel, *J. Colloid Interface Sci.* **384**, 38 (2012).
- [22] C. Largeot, C. Portet, J. Chmiola, P.-L. Taberna, Y. Gogotsi, and P. Simon, *J. Am. Chem. Soc.* **130**, 2730 (2008).
- [23] P. Simon and Y. Gogotsi, *Philos. Trans. R. Soc. A* **368**, 3457 (2010).
- [24] M. Gouy, *J. Phys. Theor. Appl.* **9** (1910).
- [25] D. L. Chapman, *Philos. Mag. Ser. 6* **25**, 475 (1913).
- [26] J. Bikerman, *Philos. Mag. Ser. 7* **33**, 384 (1942).
- [27] M. S. Kilic, M. Z. Bazant, and A. Ajdari, *Phys. Rev. E* **75**, 021502 (2007).
- [28] M. Z. Bazant, M. S. Kilic, B. D. Storey, and A. Ajdari, *Adv. Colloid Interface Sci.* **152**, 48 (2009).

- [29] D. Henderson and D. Boda, *Phys. Chem. Chem. Phys.* **11**, 3822 (2009).
- [30] R. Qiao and N. R. Aluru, *Phys. Rev. Lett.* **92**, 198301 (2004).
- [31] M. Fedorov, N. Georgi, and A. Kornyshev, *Electrochem. Commun.* **12**, 296 (2010).
- [32] R. Wang and Z.-G. Wang, *J. Chem. Phys.* **135**, 014707 (2011).
- [33] I. Kalcher, J. C. F. Schulz, and J. Dzubiella, *Phys. Rev. Lett.* **104**, 097802 (2010).
- [34] G. I. Guerrero-García, E. Gonzalez-Tovar, and M. Olvera de la Cruz, *Soft Matter* **6**, 2056 (2010).
- [35] S. Lamperski and D. Henderson, *Mol. Simul.* **37**, 264 (2011).
- [36] A. Moreira and R. Netz, in *Novel Methods in Soft Matter Simulations*, edited by M. Karttunen, A. Lukkarinen, and I. Vattulainen, Vol. 640 (Springer, Berlin, 2004), pp. 245–278.
- [37] D. Gillespie, A. S. Khair, J. P. Bardhan, and S. Pennathur, *J. Colloid Interface Sci.* **359**, 520 (2011).
- [38] A. Grosberg, T. Nguyen, and B. Shklovskii, *Rev. Mod. Phys.* **74**, 329 (2002).
- [39] R. H. French, V. A. Parsegian, R. Podgornik, R. F. Rajter, A. Jagota, J. Luo, D. Asthagiri, M. K. Chaudhury, Y.-m. Chiang, S. Granick, S. Kalinin, M. Kardar, R. Kjellander, D. C. Langreth, J. Lewis, S. Lustig, D. Wesolowski, J. S. Wettlaufer, W.-Y. Ching, M. Finnis, F. Houlihan, O. A. von Lilienfeld, C. J. van Oss, and T. Zemb, *Rev. Mod. Phys.* **82**, 1887 (2010).
- [40] Y. Levin, *Rep. Prog. Phys.* **65**, 1577 (2002).
- [41] J. J. López-García, J. Horno, and C. Grosse, *Langmuir* **27**, 13970 (2011).
- [42] Y. Lauw, M. D. Horne, T. Rodopoulos, and F. A. M. Leermakers, *Phys. Rev. Lett.* **103**, 117801 (2009).
- [43] A. J. Pascall and T. M. Squires, *Phys. Rev. Lett.* **104**, 088301 (2010).
- [44] R. Qiao and N. R. Aluru, *J. Chem. Phys.* **118**, 4692 (2003).
- [45] R. Qiao and N. R. Aluru, *Int. J. Multiscale Comput. Eng.* **2**, 173 (2004).
- [46] L. Joly, C. Ybert, E. Trizac, and L. Bocquet, *Phys. Rev. Lett.* **93**, 257805 (2004).
- [47] A. Naji, S. Jungblut, A. G. Moreira, and R. R. Netz, *Physica A* **352**, 131 (2005).
- [48] S. Vangaveti and A. Travesset, *J. Chem. Phys.* **137**, 064708 (2012).
- [49] D. A. McQuarrie, *Statistical Mechanics* (University Science Books, Sausalito, CA, 1976).
- [50] D. di Caprio, Z. Borkowska, and J. Stafiej, *J. Electroanal. Chem.* **572**, 51 (2004).
- [51] P. Biesheuvel and M. van Soestbergen, *J. Colloid Interface Sci.* **316**, 490 (2007).
- [52] V. L. Shapovalov and G. Brezesinski, *J. Phys. Chem. B* **110**, 10032 (2006).
- [53] D. J. Bonthuis, S. Gekle, and R. R. Netz, *Phys. Rev. Lett.* **107**, 166102 (2011).
- [54] M. Z. Bazant, B. D. Storey, and A. A. Kornyshev, *Phys. Rev. Lett.* **106**, 046102 (2011).
- [55] Y. Shim and H. J. Kim, *ACS Nano* **4**, 2345 (2010).
- [56] See Supplemental Material at <http://link.aps.org/supplemental/10.1103/PhysRevE.88.011301> for solving similarity variables from LDAs and tables of simulation parameters.
- [57] D. Henderson, *Prog. Surf. Sci.* **13**, 197 (1983).
- [58] S. Plimpton, *J. Comput. Phys.* **117**, 1 (1995).
- [59] J. D. Weeks, D. Chandler, and H. C. Andersen, *J. Chem. Phys.* **54**, 5237 (1971).
- [60] T. Schneider and E. Stoll, *Phys. Rev. B* **17**, 1302 (1978).
- [61] N. F. Carnahan and K. E. Starling, *J. Chem. Phys.* **51**, 635 (1969).